Abstract # 182
Parallel Session PA07
Plenary Session PL03
ALEPH 2000–069
CONF 2000–047
July 20, 2000

P R E L I M I N A R Y

Inclusive semileptonic branching ratios of b hadrons produced in Z decays

The ALEPH Collaboration

Contact person: N. Marinelli (nancy.marinelli@cern.ch)

Abstract

A new and improved measurement of the inclusive semileptonic branching ratios of the B hadrons produced in Z decay is presented, using 4 million hadronic events collected by the ALEPH detector from 1991 to 1995. Electrons and muons are selected opposite to b–tagged hemispheres. Two different methods are explored to distinguish the contributions from direct $\mathrm{b} \rightarrow \mathrm{X}\ell\nu$ and cascade $\mathrm{b} \rightarrow \mathrm{c} \rightarrow \mathrm{X}\ell\nu$ decays to the total lepton yield. One is based on the lepton transverse momentum spectrum, the other makes use of the correlation between the charge of the lepton and charge estimators built from tracks in the opposite hemisphere of the event. The latter method reduces the dependence on the modelling of the semileptonic b decays spectrum.

The results obtained by averaging the two techniques are:

$$\begin{aligned} \mathrm{BR}(\mathrm{b} \rightarrow \mathrm{X}\ell\nu) &= 0.1055 \pm 0.0009_{\,\mathrm{stat}} \pm 0.0024_{\,\mathrm{syst}} \pm 0.0021_{\,\mathrm{model}} \,, \\ \mathrm{BR}(\mathrm{b} \rightarrow \mathrm{c} \rightarrow \mathrm{X}\ell\nu) &= 0.0804 \pm 0.0014_{\,\mathrm{stat}} \pm 0.0024_{\,\mathrm{syst}} \,{}^{+0.0009}_{-0.0013}{}_{\,\mathrm{model}} \,. \end{aligned}$$

Contributed paper to ICHEP2000

1 Introduction

The value of the inclusive b hadron semileptonic branching fraction, BR(b $\to$ X$\ell\nu$), is an important parameter for heavy flavour physics: it provides an important test of the modelling of heavy hadron dynamics, and is critical for one of the measurements of the CKM matrix element $|V_{\mathrm{cb}}|$. Together with the cascade decay branching fraction, BR(b $\to$ c $\to$ X$\ell\nu$), is an important input for many heavy flavour analyses based on semileptonic final states.

Previous determinations of BR(b $\to$ X$\ell\nu$) performed at the Z and the Υ(4S) have shown some disagreement, with that measured at the Z being higher [1] while the opposite would be expected from the short b baryon lifetime [1]. On the other hand, theoretical predictions have tended to be higher than experimental measurements although recent calculations, including higher order QCD perturbative corrections, give lower values in better agreement [2, 3].

In this paper, new analyses, based on the data collected by ALEPH [4, 5] from 1991 to 1995 are presented. Two methods are used to distinguish the contributions from the direct and cascade decays to the total lepton yield. One method has better statistical precision at the expense of a dependence on the modelling of the semileptonic decays. The other is designed to have minimal decay modelling dependence. The efficiency of lepton identification is measured from data using several control samples. The description of the fragmentation of b quarks into b hadrons is based on the spectrum reconstructed with the ALEPH data [6] and is therefore independent of modelling assumptions.

2 Event samples

The analysis is based on nearly 4 million Z hadronic events selected using charged track information [7]. The statistics available for the simulation are larger than the data statistics by about a factor 2.2. Each event is divided into two hemispheres by the plane containing the interaction point and perpendicular to the thrust axis. Three samples are selected as follows.

Sample $\mathcal{B}$ A b–tagging variable ($\mathcal{B}_{\mathrm{tag}}$) based on the large mass and lifetime of b hadrons, is built as in [8] (see Figure 1). The variable is defined using tracks contained in one hemisphere, but the the primary vertex is here reconstructed using all tracks of the events, as opposed to [8]. The algorithm has good performance for events well contained in the vertex detector acceptance; events with $|\cos\theta_{\mathrm{thrust}}| > 0.7$ are rejected.

A cut $\mathcal{B}_{\mathrm{tag}} > 2$ is applied, selecting 345555 hemispheres in the data, with a b purity of 97%. The cut is about 32% efficient on b hemispheres within

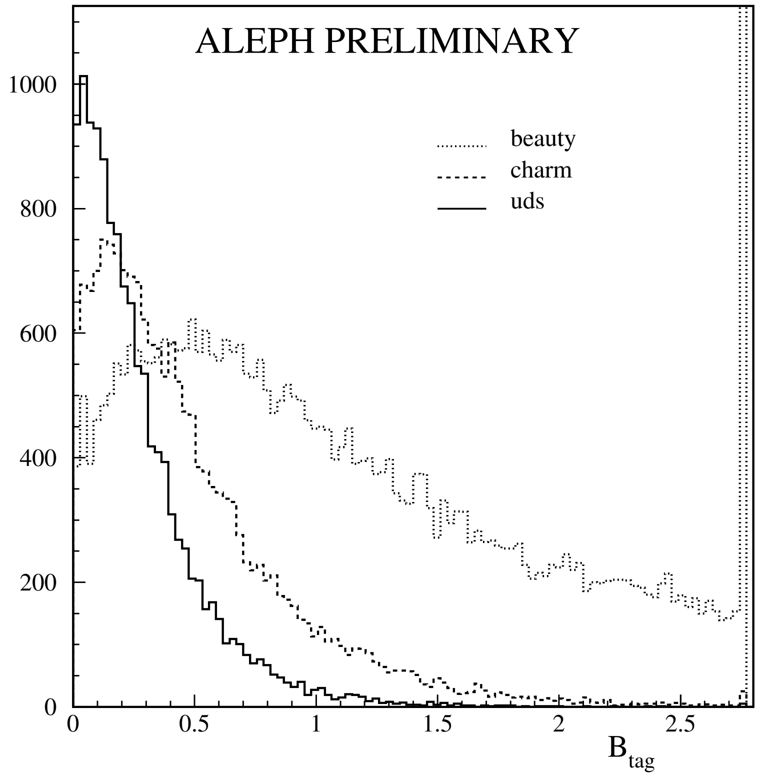

Figure 1: Distribution of the b tagging variable based on the combination of lifetime and mass information of tracks in each hemisphere opposite to a lepton candidate.

the angular region considered.

Lepton candidates (electron or muon) are searched for in hemispheres opposed to the selected ones. Events where both hemispheres are b–tagged are used twice. The candidates are ordered according to their transverse momentum, ($p_\perp$), measured with respect to the jet axis as done in [9]. When more than one lepton is found in a given hemisphere and they have opposite charge, both are used for the analysis, otherwise the one with the highest $p_\perp$ is taken.

Sample $\mathcal{P}$ In each event one of the two hemispheres is randomly chosen, and a lepton candidate, fulfilling a cut $p_\perp > 1.25$ GeV/c is searched for. This selects 148001 hemispheres in the data with an estimated b purity of 90% and a b efficiency of 12%. Since the $p_\perp$ cut suppresses cascade decays, the charge of the lepton is a good estimator of the the charge of the parent b hadron leading to a probability of tagging the charge correctly of $P_{\mathrm{b}}^{\mathcal{P}} = 0.81$, with respect to the sign of the quark at production time. As this sample does not use the vertex detector, no cut is made on $|\cos\theta_{\mathrm{thrust}}|$.

The *a priori* random choice of the hemisphere used for charge tagging ensures that there is no double counting of lepton pairs, and allows the measurement of $P_{\mathrm{b}}^{\mathcal{P}}$ from the data (see Section 6).

Lepton candidates are searched for in hemispheres opposite to the tagged ones, as in the case of the $\mathcal{B}$ sample.

Sample $\mathcal{J}$ Two hemisphere charges are calculated:

$$Q_p = \frac{\sum q\, p_{\|}^{\kappa_p}}{\sum p_{\|}^{\kappa_p}} \ ,$$

$$Q_s = \frac{\sum q\, s^{\kappa_s}}{\sum s^{\kappa_s}} \ ,$$

where the sum runs over all the good charged tracks (defined as in [7]) with momentum in excess of 200 MeV/c, q is the charge, $p_{\|}$ the component of the momentum parallel to the thrust axis, s is the impact parameter significance, defined as in [8], $\kappa_p = 0.5$ and $\kappa_s = 0.3$. Tracks with negative impact parameter are not included in the definition of Q_s.

The two charge estimators are combined using weights, w, parametrised as a function of their magnitude:

$$Q_H = w\, Q_p + [1 - w]\, Q_s \ .$$

Hemispheres are selected if they fulfil a cut $\mathcal{B}_{\mathrm{tag}} > 1.2$, which enhances the b content of the sample, and $|Q_H| > 0.2$. This ensures a good probability that the sign of Q_H is correlated with the charge of the b quark in the parent b hadron. Since the $\mathcal{B}_{\mathrm{tag}}$ variable is used, events with $|\cos\theta_{\mathrm{thrust}}| > 0.7$ are not considered. Hemispheres containing a lepton candidate with $p_{\perp} > 1.25$ GeV/c are rejected in order to keep this sample statistically independent of sample $\mathcal{P}$.

The procedure selects 392523 hemispheres in the data with an estimated b purity of 87% and a b efficiency of 32%. The probability of correct b charge tagging is $P_{\mathrm{b}}^{\mathcal{J}} = 0.73$.

The lepton yield in hemispheres opposite to the selected ones is studied as for the previous samples.

3 Lepton identification

The identification of electrons and muons follows the lines of [9]. A good control of the identification efficiency, as well as of the background in the selected sample is crucial for this analysis. A reduced dependence on the description of the b fragmentation is achievable if the acceptance is extended to low momentum leptons and, for this reason, some of the selection cuts have been revised.

The main change is, however, the use of a new estimator for the charged particle energy loss in the Time Projection Chamber (TPC). In the recent reprocessing of the LEP1 data sample, information from the pulse height measured by the TPC pads has been used to build a similar estimator to the one for the wire measurements. The pad estimator is available for all tracks, while the wire estimator is calculated only for tracks that have a minimum number of isolated wire signals, which leads to an average inefficiency of about 15% in hadronic environment.

From those two a new energy loss estimator I is built; this coincides with the pad estimator for tracks that do not fulfil the requirement on the minimum number of isolated wire signals, and combines wire and pad information otherwise.

3.1 Electrons

Compared to the selection described in [9], the momentum cut is lowered to $p > 2$ GeV/c.

The requirement on the minimum number of isolated TPC wire signals is dropped, and a cut on the new energy loss estimator $I > -2$ is applied. This removes the dependence of the identification efficiency upon the track isolation, and hence the electron $p_{\perp}$. Compared to the previous selection, the new treatment of the energy loss information provides an increase in efficiency that goes from a few percent at high $p_{\perp}$ to about 30% at low $p_{\perp}$. The background increases marginally.

3.2 Muons

The momentum cut is lowered to $p > 2.5$ GeV/c. This still ensures that most muons reach the muon chambers, although the small dependence on the momentum which this causes has required a dedicated study.

An cut on the polar angle $|\cos\theta| < 0.69$ is applied, which ensures that the muon is within the acceptance of both vertex detector layers. At least one VDET hit is required to be associated with the muon track, and the distance to the primary vertex in the $x - y$ plane is required to be $|d_0| < 2.5$ mm. This substantially reduces the contamination from muons coming from kaon and pion decays.

In addition a cut on the energy loss estimator $I > -2$ is applied; this further reduces the background from decaying kaons by more than a factor of two.

4 The analysis method

4.1 Transverse momentum analysis

With sample $\mathcal{B}$ described in Section 2, a large number of nearly unbiased b decays is selected. The lepton rate in such a sample can be directly interpreted in terms of the sum of the direct and cascade inclusive semileptonic b decays, weighted with their selection efficiencies, once contributions from other physics sources and misidentified leptons have been corrected for.

The study of the lepton rate as a function of the transverse momentum which discriminates the two components, allows the two branching ratios to be fitted simultaneously.

Therefore a measurement of BR(b $\rightarrow$ X$\ell\nu$) and BR(b $\rightarrow$ c $\rightarrow$ X$\ell\nu$) can be obtained from a binned likelihood fit to the expected number of events in each transverse momentum interval, as follows:

$$\mathcal{L} \;=\; \prod_i \frac{e^{-\mu_i}\;\mu_i^{n_i}}{n_i!}\;, \tag{1}$$

where the product runs over the transverse momentum bins, n_i is the number of leptons found in the data in each bin, μ_i is the number of expected leptons, which depends on the two branching ratios and contains the contributions from all the other sources of lepton candidates.

Equation 1 can be rewritten in the following way, mathematically equivalent:

$$\mathcal{L} \;=\; \underbrace{\frac{e^{-\mu}\;\mu^N}{N!}}_{\text{counting}} \;\times\; \underbrace{\prod_{j=1}^{N} \mathcal{F}(p_\perp^j)}_{p_\perp\ \text{spectrum}}\;, \tag{2}$$

where N is the total number of candidates observed in the data ($N = \sum_i n_i$), μ is the expected number ($\mu = \sum_i \mu_i$), and $\mathcal{F}(p_\perp)$ is the binned function which gives the expected shape of the distribution of the candidates as a function of $p_\perp$ ($\mathcal{F}_i = \mu_i/\mu$). The product runs over the lepton candidates.

The part of the likelihood labelled as "counting" contains the information on the total rate, and is therefore sensitive to the (weighted) sum of the two branching ratios. It is affected by uncertainties in the lepton identification efficiency and background, and has little dependence on the modelling of the $p_\perp$ spectrum.

The part labelled as "$p_\perp$ spectrum" is sensitive to the relative contribution of the two signal sources, but almost insensitive to their absolute value. It is heavily affected by uncertainties in the b decay modelling.

4.2 Charge correlation analysis

Another way of discriminating the b $\rightarrow$ X$\ell\nu$ and b $\rightarrow$ c $\rightarrow$ X$\ell\nu$ components is to exploit the different correlation with the parent quark charge. The second part of the likelihood in Equation 2 can be replaced with a term containing the fraction of leptons that have same or opposite charge relative to a charge estimator built using tracks in the opposite hemisphere (*e.g.* jet charge).

However, if such a method was applied to sample $\mathcal{B}$ that would result in a poor statistical power. For this purpose the charge tag samples $\mathcal{P}$ and $\mathcal{J}$ have been selected, relaxing the requirement on the b purity in favour of higher statistic.

A likelihood function can be written combining the counting part from sample $\mathcal{B}$ and the charge spectra of samples $\mathcal{P}$ and $\mathcal{J}$ as follows:

$$\mathcal{L} = \underbrace{\frac{e^{-\mu}\,\mu^N}{N!}}_{\text{counting }(\mathcal{B})} \times \underbrace{\mathcal{F_P}^{N_{O_\mathcal{P}}}(1-\mathcal{F_P})^{N_{S_\mathcal{P}}}}_{\text{charge }(\mathcal{P})} \times \underbrace{\mathcal{F_J}^{N_{O_\mathcal{J}}}(1-\mathcal{F_J})^{N_{S_\mathcal{J}}}}_{\text{charge }(\mathcal{J})}, \quad (3)$$

where $\mathcal{F_P}$ is the expected fraction of lepton candidates with the charge opposite to the charge tag of the other hemisphere in sample $\mathcal{P}$, $N_{O_\mathcal{P}}$ and $N_{S_\mathcal{P}}$ are the number of candidates with opposite and same charge found in the data. The same holds for sample $\mathcal{J}$.

The expected fractions $\mathcal{F_P}$ and $\mathcal{F_J}$ are sensitive to the relative contribution of the $\mathrm{b} \to \mathrm{X}\ell\nu$ and $\mathrm{b} \to \mathrm{c} \to \mathrm{X}\ell\nu$ components and depend on the rate of correct tagging for the opposite hemisphere charge estimator, as well as on the background components.

5 Flavour composition of the selected samples

The flavour composition for the three samples used is estimated as follows.

The fraction F_{hemi} of single tagged hemispheres is measured from the data. The efficiency for tagging charm events, ϵ_{c}, and the average efficiency for tagging light quark events, ϵ_{x}, are measured on simulated events, and the sample composition is calculated as:

$$\begin{aligned} f^{\mathrm{b}}_{\mathrm{hemi}} &= 1 - \frac{R_{\mathrm{c}}\epsilon_{\mathrm{c}} + (1 - R_{\mathrm{b}} - R_{\mathrm{c}})\epsilon_{\mathrm{x}}}{F_{\mathrm{hemi}}}, \\ f^{\mathrm{c}}_{\mathrm{hemi}} &= \frac{R_{\mathrm{c}}\epsilon_{\mathrm{c}}}{F_{\mathrm{hemi}}}, \\ f^{\mathrm{x}}_{\mathrm{hemi}} &= \frac{(1 - R_{\mathrm{b}} - R_{\mathrm{c}})\,\epsilon_{\mathrm{x}}}{F_{\mathrm{hemi}}}, \end{aligned}$$

where R_{b} and R_{c} are the ratios of the $\mathrm{b\bar{b}}$ and $\mathrm{c\bar{c}}$ partial widths of the Z to the total hadronic width, taken from experimental measurements.

6 Charge tagging in samples $\mathcal{P}$ and $\mathcal{J}$

The terms $\mathcal{F_P}$ and $\mathcal{F_J}$ in Equation 3 are written in terms of the probabilities that the charge of the parent quark in the hemisphere opposite to the lepton candidate considered is correctly tagged.

These probabilities for b quarks are measured from the data, using a double–tag method. The description below applies to both samples $\mathcal{P}$ and $\mathcal{J}$.

The selection cut is applied to both hemispheres, and the probability of tagging correctly the b quark charge, P_{b}, is related to the fraction of opposite charge hemispheres in b events, $F_{\mathrm{b}}^{\mathrm{oc}}$, as follows:

$$F_{\mathrm{b}}^{\mathrm{oc}} = P_{\mathrm{b}}^2(1+\rho_1) + (1-P_{\mathrm{b}})^2(1+\rho_2) \ , \tag{4}$$

where ρ_1 and ρ_2 account for correlations between the tagging probabilities in the two hemispheres. Allowing $\rho_1 \neq \rho_2$ describes the fact that the total charge of the events is on average nonzero, due to the interaction of particles with the matter of the detector.

The quantity measured in the data is the fraction F^{oc} of opposite charge hemispheres in the selected sample, which can be written as:

$$F^{\mathrm{oc}} = f_{\mathrm{evt}}^{\mathrm{b}} F_{\mathrm{b}}^{\mathrm{oc}} + f_{\mathrm{evt}}^{\mathrm{c}} F_{\mathrm{c}}^{\mathrm{oc}} + f_{\mathrm{evt}}^{\mathrm{x}} F_{\mathrm{x}}^{\mathrm{oc}} \ , \tag{5}$$

where $f_{\mathrm{evt}}^{\mathrm{b}}$, $f_{\mathrm{evt}}^{\mathrm{c}}$ and $f_{\mathrm{evt}}^{\mathrm{x}}$ are the contributions of b, c and light flavour events to this sample. These fractions are measured with the same procedure used to estimate the hemisphere sample composition (Section 5):

$$\begin{aligned}
f_{\mathrm{evt}}^{\mathrm{b}} &= 1 - \frac{R_{\mathrm{c}}\zeta_{\mathrm{c}} + (1-R_{\mathrm{b}}-R_{\mathrm{c}})\zeta_{\mathrm{x}}}{F_{\mathrm{evt}}} \ , \\
f_{\mathrm{evt}}^{\mathrm{c}} &= \frac{R_{\mathrm{c}}\zeta_{\mathrm{c}}}{F_{\mathrm{evt}}} \ , \\
f_{\mathrm{evt}}^{\mathrm{x}} &= \frac{(1-R_{\mathrm{b}}-R_{\mathrm{c}})\,\zeta_{\mathrm{x}}}{F_{\mathrm{evt}}} \ ,
\end{aligned} \tag{6}$$

where F_{evt} is the fraction of events with both hemispheres tagged in the data, ζ_{c} and ζ_{x} are the charm and light quark event efficiencies in the simulation.

The fractions of events with opposite charge hemispheres in charm and light quark events $F_{\mathrm{c}}^{\mathrm{oc}}$ and $F_{\mathrm{x}}^{\mathrm{oc}}$ are taken from the simulation, and Equation 5 is solved for $F_{\mathrm{b}}^{\mathrm{oc}}$. This is then used in Equation 4 to calculate P_{b}.

7 Sources of systematic errors

In this section the sources of possible systematic uncertainty investigated for the two analyses will be described. The estimated errors are listed in Table 2 at the end of the paper.

7.1 Z partial widths to $\mathrm{b\bar{b}}$ and $\mathrm{c\bar{c}}$

The values of R_{b} and R_{c} are used in the derivation of the sample compositions of the three hemisphere samples, and in the calculation of $P_{\mathrm{b}}^{\mathcal{P}}$ and $P_{\mathrm{b}}^{\mathcal{J}}$.

The most recent LEP/SLD averages are used [10], $R_\mathrm{b} = 0.21643 \pm 0.00073$ and $R_\mathrm{c} = 0.1694 \pm 0.0038$, and the estimated uncertainties are considered as sources of systematic error.

7.2 Heavy quarks from gluon splitting

Charm and bottom quark pairs may be produced from a gluon splitting process. The heavy flavour hadrons resulting from this process have a significantly softer energy spectrum and thus give rise to a source of prompt leptons with kinematic properties substantially different from those produced by heavy hadrons from direct Z decay. In addition, leptons originating from gluons splitting to heavy quarks have a random charge correlation with the charge estimators defined in the opposite hemisphere.

The latest world average values are used for the number of gluons splitting to heavy quarks per hadronic Z decay [12],

$$\begin{aligned} N(\mathrm{g} \to \mathrm{b\bar{b}}) &= 0.00318 \pm 0.00046 \ , \\ N(\mathrm{g} \to \mathrm{c\bar{c}}) &= 0.0251 \ \ \pm 0.063 \ , \end{aligned}$$

and the experimental errors are used to estimate the associated uncertainty.

7.3 Muon identification efficiency and background

The identification efficiency for high energy muons is measured from data using Z decays to muon pairs, as a function of polar and azimuthal angle. Simulated events are reweighted to reproduce the measured efficiencies. Correction factors are typically a few permille.

Simulated events show that some dependence of the identification efficiency upon the muon momentun appears for momenta around 3 GeV/c. This effect is also checked on real data using $\gamma\gamma \to \mu^+\mu^-$ events. Additional correction factors, of order $1 \div 2\%$ are derived for muons with momenta between 2.5 GeV/c and 4 GeV/c.

The systematic error on the efficiency is estimated by performing the measurement without the correction factors.

The main background for muon candidates is given by misidentified pions as well as pions decaying before entering the calorimeters. The corresponding contributions for kaons are substantially reduced by the cut on the measured energy loss, and are estimated to be a factor of four smaller.

In order to check the background rate from data, $\mathrm{K^0_S} \to \pi^+\pi^-$ decays are selected in hadronic events to yield a 99% pure sample of pions. The muon identification procedure is applied to these tracks, and the selection efficiency is compared between data and Monte Carlo. Agreement is found within the statistical precision of the test, which is 5%. The test is repeated applying different $\mathcal{B}_\mathrm{tag}$ cuts in the hemisphere opposite to the $\mathrm{K^0_S}$ candidate in order to check for a possible dependence on the flavour. No trend is observed.

The uncertainty of 5% estimated for the check with $\mathrm{K^0_S} \to \pi^+\pi^-$ is enlarged to 10% for the assignment of a systematic error to the muon background. This allows additional uncertainties from the smaller kaon component, as well as possible differences between data and simulation in the production rates and kinematic properties of pions and kaons in b events.

7.4 Electron identification efficiency and background

The electron identification efficiency is measured from data using photon conversions in the detector material. Correction factors are derived, with respect to the Monte Carlo for the dependence on momentum, transverse momentum and polar angle. These factors typically differ from unity by less than 1%. The associated systematic uncertainty is estimated by removing the corrections.

The background from hadron misidentification is estimated by removing the cut on the energy loss, and studying the shape of the I estimator, given by the electron Gaussian, centred on zero, and the hadron component at negative values. No significant deviation is observed, and an uncertainty of 20% is assigned from the statistical precision of the method.

The background from unidentified photon conversions is estimated by studying from the shape of the variable

$$\rho_\gamma \ = q\, d_0\, p_\perp^{\mathrm{beam}} \ ,$$

where q is the charge of the lepton, d_0 is the signed distance of minimal approach to the primary vertex in the $x-y$ plane and $p_\perp^{\mathrm{beam}}$ is the component of the track momentum transverse to the beam axis. The variable ρ_γ is expected to be zero for prompt electrons and proportional to the materialization radius for electrons coming from photon conversions. The study of the positive tail of the distribution yields a correction factor of 1.05 to be applied to the simulation, with a statistical error of 0.02. The correction factor is removed to estimate the systematic uncertainty.

7.5 Two lepton final states

The $\mathrm{b} \to \mathrm{c} \to \mathrm{X}\ell\nu$ rate is in principle different in transitions where the W from the b hadron decays leptonically, $\mathrm{BR}(\mathrm{b}\to\mathrm{c}\to\mathrm{X}\ell\nu)|_\ell$, or hadronically, $\mathrm{BR}(\mathrm{b}\to\mathrm{c}\to\mathrm{X}\ell\nu)|_\mathrm{h}$. The fit could yield a biased result for the average $\mathrm{BR}(\mathrm{b}\to\mathrm{c}\to\mathrm{X}\ell\nu)$ if the acceptance were different for the two cases. This effect is investigated by changing in the simulation the relative population of the two species and recalculating all efficiencies and spectra. The $\mathrm{BR}(\mathrm{b}\to\mathrm{c}\to\mathrm{X}\ell\nu)|_\ell$ is increased by 20% and the $\mathrm{BR}(\mathrm{b}\to\mathrm{c}\to\mathrm{X}\ell\nu)|_\mathrm{h}$ is decreased accordingly. The shift observed in the fitted values is taken as an estimate of the associated systematic error.

7.6 Other sources of prompt leptons

The rate of leptons coming from J/ψ and from intermediate τ decays used for this analysis are;

$$\begin{aligned} \mathrm{BR}(\mathrm{b} \to \mathrm{J}/\psi \to \ell\ell) &= 0.0121 \quad \pm 0.0015 \text{ [10]} , \\ \mathrm{BR}(\mathrm{b} \to \tau \to \ell) &= 0.00452 \pm 0.00074 \text{ [1]} . \end{aligned}$$

Leptons produced from cascade b decays where the intermediate charm is produced from a W $\to$ $\bar{\mathrm{c}}$s transition, denoted b $\to$ W $\to$ $\bar{\mathrm{c}}$ $\to$ ℓ, are also a background to the analysis. They affect most directly the result for BR(b $\to$ c $\to$ X$\ell\nu$) in the transverse momentum analysis, since they have kinematic properties similar to b $\to$ c $\to$ X$\ell\nu$ decays. On the contrary in the charge correlation analysis only the value of BR(b $\to$ X$\ell\nu$) depends on the rate of these transitions since the correlation between the charge of the lepton and the charge of the parent quark is the same as in b $\to$ X$\ell\nu$ direct decays. The value used is [10]:

$$\mathrm{BR}(\mathrm{b} \to \mathrm{W} \to \bar{\mathrm{c}} \to \ell) = 0.0162 \pm 0.0044 .$$

The residual background of c$\bar{\mathrm{c}}$ events contributes to the total observed lepton yield with the semileptonic decays of charmed hadrons. The LEP average value [12] is taken:

$$\mathrm{BR}(\mathrm{c} \to \ell) = 0.0985 \pm 0.0032 .$$

All the sources of leptons previuosly described are subtracted by the total lepton yield.

The rate of leptons coming from charmless semileptonic b decays, b $\to$ $\mathrm{X_u}\ell$, mainly affects the region at high $p_\perp$ in the spectrum. A variation of its relative proportion with respect to the total BR(b $\to$ X$\ell\nu$) has to be allowed. The value used in this analysis is [11]:

$$\mathrm{BR}(\mathrm{b} \to \mathrm{X_u}\ell) = 0.00167 \pm 0.00055 .$$

7.7 Fragmentation of b quarks

The mean scaled energy spectrum of b hadrons in the simulation is modified in order to reproduce the spectrum reconstructed in the model–independent analysis of [6].

The stastitical and systematic uncertainty on the population of each energy bin is propagated to the measured branching ratios, taking into account bin–to–bin correlations. The systematic errors on the energy spectrum due to the uncertainty on the charmed meson species produced in B meson decays are not considered here, since they are correlated with the uncertainty on the modelling of semileptonic decays (see later Section 7.14).

The correction factors derived from the comparison of the measured and simulated energy spectra of B mesons are applied also to $\mathrm{B_s^0}$ mesons and b baryons.

7.8 Fragmentation of c quarks

Charm fragmentation is simulated using the PSSZ [13] model. The parameter ε_{c}, which controls the shape of the function is set to $\varepsilon_{\mathrm{c}} = 0.039 \pm 0.008$ which corresponds to a value of the mean scaled energy of weakly–decaying charmed hadrons, $\langle X_{\mathrm{c}} \rangle = 0.484 \pm 0.008$ [10]. The systematic error is calculated varying ε_{c} within the quoted uncertainty.

7.9 Charm and light quark background

The calculation of the sample compositions described in Section 5 relies on the simulation for the estimate of the charm and light quark hemisphere selection efficiencies.

For samples $\mathcal{B}$ and $\mathcal{J}$ the estimate of the uncertainty on the background efficiencies follows the lines of [8]. The values used are:

$$\begin{aligned} \epsilon_{\mathrm{c}}^{\mathcal{B}} &= 0.00939 \pm 0.00094 \qquad & \epsilon_{\mathrm{x}}^{\mathcal{B}} &= 0.00060 \pm 0.00015 \ , \\ \epsilon_{\mathrm{c}}^{\mathcal{J}} &= 0.0439 \pm 0.0022 \qquad & \epsilon_{\mathrm{x}}^{\mathcal{J}} &= 0.0054 \pm 0.0008 \ . \end{aligned}$$

For sample $\mathcal{P}$ the dominant sources of uncertainty are the charm semileptonic branching fraction and decay modelling, for charm hemispheres, and lepton background for light quark hemispheres. The corresponding values are

$$\epsilon_{\mathrm{c}}^{\mathcal{P}} = 0.0108 \pm 0.0011 \qquad \epsilon_{\mathrm{x}}^{\mathcal{P}} = 0.0016 \pm 0.0003 \ .$$

7.10 Charge tagging in charm and light quark hemispheres

The fraction of opposite charge charm and light quark hemispheres entering Equation 5 is taken from the simulation.

For charm hemispheres, the correlation between the charge of the quark and the sign of the estimator is stronger than in the case of bottom hemispheres. In sample $\mathcal{P}$ this is primarily due to neutral B meson mixing and cascade semileptonic b decays which dilute the correlation. In the case of sample $\mathcal{J}$ it is mainly due to the higher charm quark charge. The systematic uncertainty from this source is evaluated by setting the charge correlation for charm hemispheres equal to the one of bottom hemispheres, and taking half of the difference as systematic uncertainty.

In light quark events, $F_{\mathrm{x}}^{\mathrm{oc}}$ is still somewhat larger than 0.5 due to the correlation of the estimator with the parent quark charge, for both samples.

However the systematic uncertainty obtained by setting it equal to 0.5 is negligible.

7.11 Charge tagging in b hemispheres

Besides the sources already considered, the uncertainty on P_{b} also depends on the uncertainties on F^{oc}, F_{evt}, ρ_1, ρ_2, ζ_{c} and ζ_{x} appearing in Equations 4-6.

The statistical errors on F^{oc} and F_{evt} are propagated to the results of the fit and included in the statistical errors on the branching ratios.

The values of ρ_1 and ρ_2 measured in the simulated events are 2.4% and 2.6% for the $\mathcal{J}$ sample, 1.8% and -0.4% for the $\mathcal{P}$ sample. The associated systematic uncertainty is estimated by setting them to zero taking half of the shift observed.

The uncertainties from ζ_{c} and ζ_{x}, which are measured from the simulation, are negligible.

7.12 Neutral B meson mixing

The mixing of neutral B mesons contributes to the degradation of the correlation between the charge of the lepton and the charge of the parent b quark produced in the Z decay. The LEP average $\bar{\chi} = 0.1186 \pm 0.0043$ [12] is used as input in the likelihood. This value is interpreted as the average mixing rate for the b hadron mixture from $\mathrm{b} \to \mathrm{X}\ell\nu$ decays.

The relative population of $\mathrm{B}^0_{\mathrm{d}}$ and B^+ mesons is not equal in $\mathrm{b} \to \mathrm{c} \to \mathrm{X}\ell\nu$ decays, due to the different semileptonic branching ratios of D^+ and D^0 mesons, leading to an effectively higher value of the average mixing parameter $\bar{\chi}\prime = \bar{\chi}\,(1+\delta)$. The value of δ is estimated from the simulation $\delta = 0.13$ and is varied by 50% for the systematic uncertainty.

As a consequence the expected fraction of events with hemispheres of opposite sign for the $\mathrm{b} \to \mathrm{X}\ell\nu$ and $\mathrm{b} \to \mathrm{c} \to \mathrm{X}\ell\nu$ components is:

$$\begin{aligned} \mathrm{b} \to \mathrm{X}\ell\nu: \quad & \mathcal{F} = P_{\mathrm{b}}\,(1-\bar{\chi}) + (1-P_{\mathrm{b}})\,\bar{\chi}\ , \\ \mathrm{b} \to \mathrm{c} \to \mathrm{X}\ell\nu: \quad & \mathcal{F} = P_{\mathrm{b}}\,\bar{\chi}\prime + (1-P_{\mathrm{b}})\,(1-\bar{\chi}\prime)\ . \end{aligned}$$

7.13 Charge correlation for lepton background

Leptons coming from kaon and pion decays in flight as well as misidentified kaons and pions retain some information about the charge of the primary quark, both in charm and in beauty events and they have to be taken into account when evaluating the opposite charge and same charge fractions in the charge correlation analysis. The rate at which the information about the quark charge is retained is measured in the Monte Carlo. The sistematic uncertainty is evaluated by setting it at 50% and dividing by two the effect. The variation is performed indipendently for K and π.

7.14 Modelling of direct semileptonic b decays

B^0 and B^+ mesons decay semileptonically into D, $D^\star$ and $D^{\star\star}$ mesons. Leptons coming from each of these components have a different energy spectrum so that the shape of the inclusive $B^{0(+)} \to \ell^- \overline{\nu}$ X spectrum depends on the branching fractions of B^0 and B^+ into the various charmed species.

Process	BR (%)
$B \to D\ell\nu$	1.95 ± 0.27
$B \to D^\star\ell\nu$	5.05 ± 0.25
$B \to D^{\star\star}\ell\nu$	2.7 ± 0.7
$B \to D_1\ell\nu$	0.63 ± 0.11
$B \to D_2^\star\ell\nu$	0.23 ± 0.09

Table 1: Branching ratios for semileptonic decays of B mesons with different charmed mesons in the final state.

The simulated fractions of D, $D^\star$, D_1, $D_2^\star$ are reweighted using the latest measured value (see Table 1). The broad $D^{\star\star}$ states are assumed to be equal to the sum of the narrow D_1 and $D_2^\star$ states, and the non resonant $D^{(\star)}\pi$ decays account for the rate needed in order to add up to the measured inclusive $D^{\star\star}$ branching ratio.

The systematic uncertainty is evaluated by varying the measured branching fractions within their estimated errors. Additionally the rate of the broad states is set to zero and compensated entirely with the non–resonant $D^{(\star)}\pi$ states. In each case, the B meson energy spectrum measured in [6] is used, so taking correctly into account the correlation between the two analyses. Finally, the observed shifts in the measured branching ratios are symmetrized, added in quadrature, and enlarged by 25% to account for the additional B_s^0 and b baryon states.

The lepton energy spectra obtained with this procedure are compared in Fig. 2 with the spectra given in [14]. In Fig. 3 the effect of the corrections applied to estimate the systematic is shown. The spectra resulting from this semi–exclusive treatment always lie within the softest (ISGW**) and hardest (ISGW) spectra.

7.15 Modelling of $c \to \ell$ and $b \to c \to X\ell\nu$ decays

The $c \to \ell$ decay spectrum is obtained by a combined fit to DELCO [15] and MARK III [16] data is performed using the ACCMM model and varied as described in [14].

As for the $b \to c \to X\ell\nu$, it is a two step process and the experimental situation is less clear. The model proposed for $c \to \ell$ is combined with the measured $b \to D$ spectrum from CLEO [17] following what is done in [14].

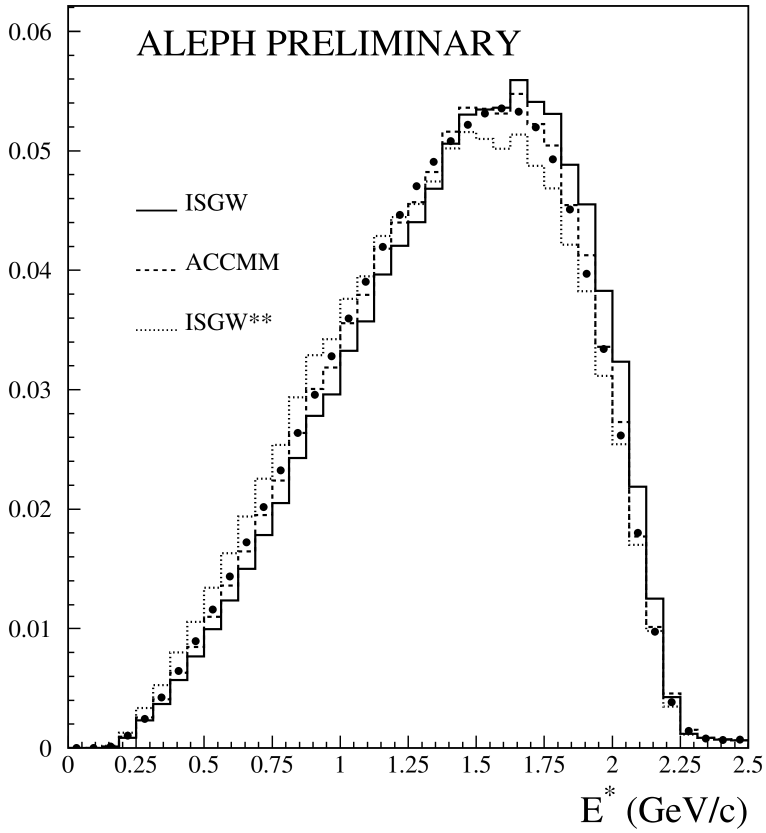

Figure 2: Lepton energy spectrum in the b rest frame. The histograms show the distributions obtained after reweighting with the ACCMM, ISGW and ISGW** models. The dots show the spectrum after correcting the Monte Carlo by following the procedure described in Section 7.14 using the central value of the branching ratios listed in Table 1.

8 Results

The results obtained with the transverse momentum analysis and the fit to the $p_\perp$ spectrum are the following:

$$
\begin{aligned}
\mathrm{BR}(\mathrm{b} \to \mathrm{X}\ell\nu) &= 0.1092 \pm 0.0007_{\mathrm{stat}} \pm 0.0016_{\mathrm{syst}} \pm 0.0039_{\mathrm{model}} \;, \\
\mathrm{BR}(\mathrm{b} \to \mathrm{c} \to \mathrm{X}\ell\nu) &= 0.0733 \pm 0.0010_{\mathrm{stat}} \pm 0.0042_{\mathrm{syst}} \pm 0.0039_{\mathrm{model}} \;.
\end{aligned}
$$

while the method based on the charge correlation analysis gives:

$$
\mathrm{BR}(\mathrm{b} \to \mathrm{X}\ell\nu) = 0.1039 \pm 0.0011_{\mathrm{stat}} \pm 0.0030_{\mathrm{syst}} \pm 0.0013_{\mathrm{model}} \;,
$$

ALEPH PRELIMINARY

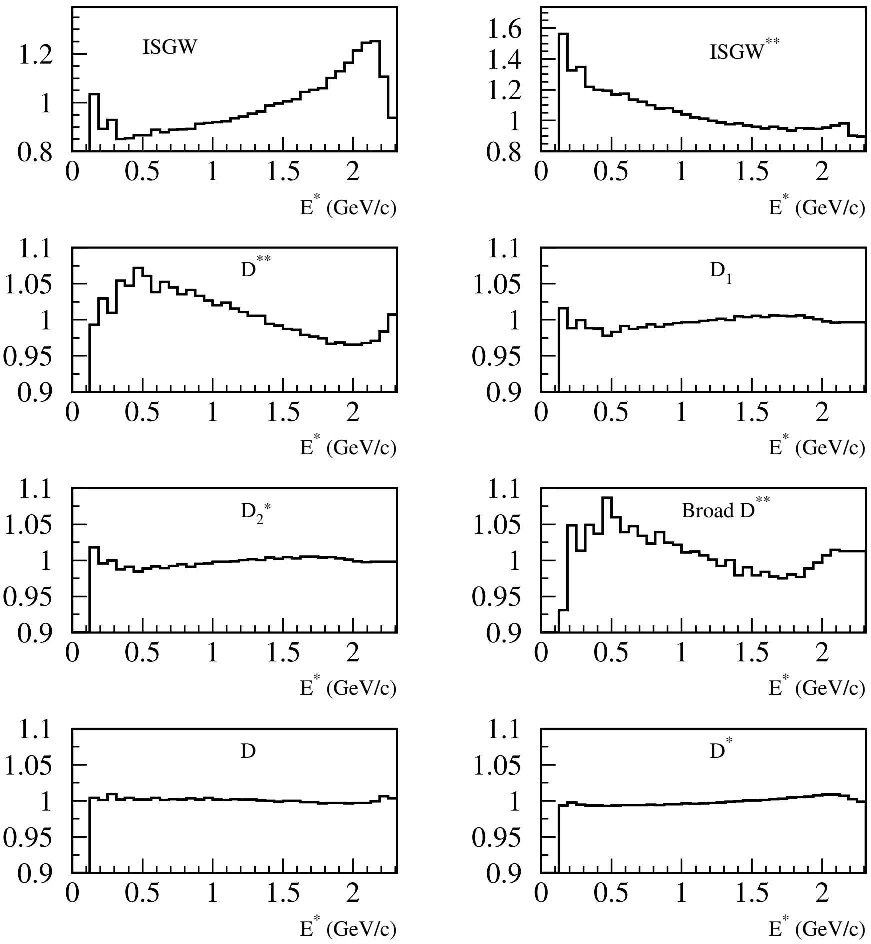

Figure 3: The two plots on top show the ratio between the ISGW (ISGW**) model and the spectrum obtained by correcting the Monte Carlo using the central value of the branching ratios listed in Table 1. The next six histograms show the effect on the spectrum due to the variation of each component with respect to the central value.

$$\mathrm{BR}(\mathrm{b} \to \mathrm{c} \to \mathrm{X}\ell\nu) \quad = \quad 0.0817 \pm 0.0015_{\,\mathrm{stat}} \pm 0.0024_{\,\mathrm{syst}}\ {}^{+0.0008}_{-0.0013}{}_{\,\mathrm{model}}\ .$$

The two methods are consistent within 1.4 σ of the total error and their average is then considered. The preliminary ALEPH results are:

$$\begin{aligned}\mathrm{BR}(\mathrm{b} \to \mathrm{X}\ell\nu) &= 0.1055 \pm 0.0009_{\,\mathrm{stat}} \pm 0.0024_{\,\mathrm{syst}} \pm 0.0021_{\,\mathrm{model}}\ ,\\ \mathrm{BR}(\mathrm{b} \to \mathrm{c} \to \mathrm{X}\ell\nu) &= 0.0804 \pm 0.0014_{\,\mathrm{stat}} \pm 0.0024_{\,\mathrm{syst}}\ {}^{+0.0009}_{-0.0013}{}_{\,\mathrm{model}}\ .\end{aligned}$$

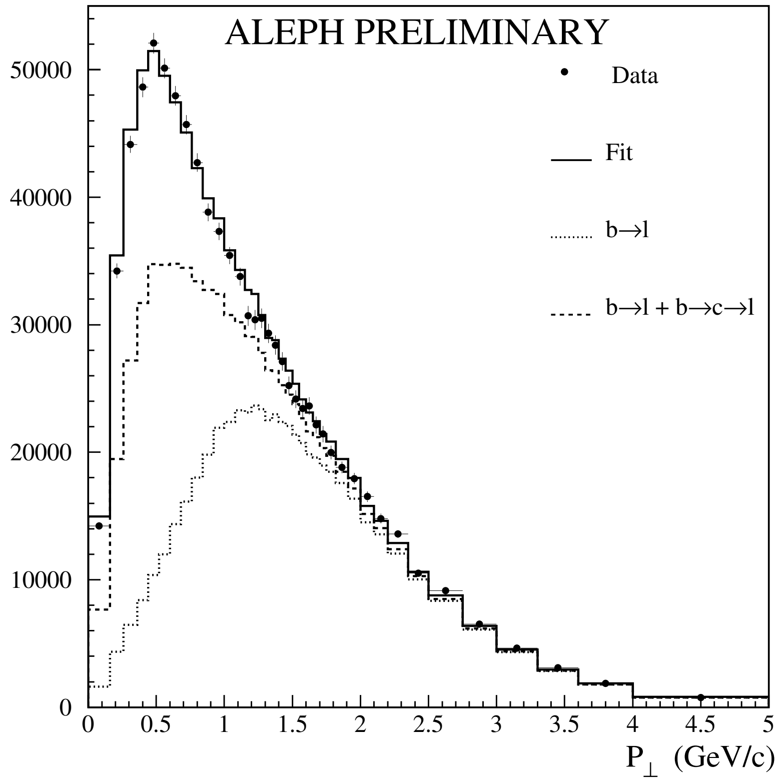

Figure 4: Comparison between the $p_\perp$ spectrum measured in the data and the result of the fit. The contribution from $\mathrm{b} \to \mathrm{X}\ell\nu$ as well as the sum of $\mathrm{b} \to \mathrm{X}\ell\nu$ and $\mathrm{b} \to \mathrm{c} \to \mathrm{X}\ell\nu$ are shown.

References

[1] Review of Particle Physics, C. Caso *et al.*, (Particle Data Group), Eur. Phys. J. C **3** (1998) 1.

[2] E. Bagan, P. Ball, V.M. Braun and P. Gosdzinsky, Nucl. Phys. B **432** (1994) 3; E. Bagan, P. Ball, V.M. Braun and P. Gosdzinsky, Nucl. Phys. Lett B **342** (1995) 362; E. Bagan, P. Ball, B. Fiol and P. Gosdzinsky, Nucl. Phys. Lett B **351** (1995) 546.

[3] M. Neubert, C.T. Sachrajda, Nucl. Phys. B **483** (1997) 339.

[4] ALEPH Coll., D. Decamp et al., Nucl. Instr. Meth. A **294** (1990) 121.

	Δ[BR(b $\rightarrow$ X$\ell\nu$)]		Δ[BR(b $\rightarrow$ c $\rightarrow$ X$\ell\nu$)]	
Source	Charge	$p_\perp$	Charge	$p_\perp$
BR(c $\rightarrow \ell$)	$\mp$ 0.015	negl	$\pm$ 0.015	$\mp$ 0.009
BR(b $\rightarrow$ W $\rightarrow \bar{c} \rightarrow \ell$)	$\mp$ 0.205	$\pm$ 0.009	$\mp$ 0.035	$\mp$ 0.370
BR(b $\rightarrow \tau \rightarrow \ell$)	$\mp$ 0.058	$\mp$ 0.022	$\mp$ 0.015	$\mp$ 0.072
BR(b $\rightarrow$ u)	$\mp$ 0.028	$\mp$ 0.041	$\mp$ 0.005	$\pm$ 0.016
BR(b $\rightarrow$ c $\rightarrow$ X$\ell\nu$)$\|_\ell$	$\pm$ 0.022	$\pm$ 0.004	$\mp$ 0.019	$\pm$ 0.008
BR(b $\rightarrow$ J/$\psi \rightarrow \ell\ell$)	$\mp$ 0.006	$\mp$ 0.014	$\mp$ 0.009	$\pm$ 0.005
b fragmentation	$\mp$ 0.119	$\mp$ 0.104	$\mp$ 0.111	$\mp$ 0.132
c fragmentation	$\pm$ 0.005	$\pm$ 0.001	$\mp$ 0.005	negl
$R_{\rm b}$	negl.	negl	0	negl
$R_{\rm c}$	$\mp$ 0.007	$\pm$ 0.006	$\pm$ 0.018	$\mp$ 0.002
N(g $\rightarrow$ b$\bar{\rm b}$)	$\mp$ 0.002	$\mp$ 0.002	$\mp$ 0.001	$\mp$ 0.001
N(g $\rightarrow$ c$\bar{\rm c}$)	$\mp$ 0.009	$\mp$ 0.001	$\mp$ 0.010	$\mp$ 0.023
electron ID efficiency	$\mp$ 0.080	$\mp$ 0.061	$\mp$ 0.056	$\mp$ 0.086
muon ID efficiency	$\pm$ 0.063	$\pm$ 0.065	$\pm$ 0.039	$\pm$ 0.039
γ conversions	$\mp$ 0.006	$\pm$ 0.003	$\mp$ 0.008	$\mp$ 0.022
electron bkg	$\mp$ 0.007	$\pm$ 0.004	$\mp$ 0.009	$\mp$ 0.026
muon bkg	$\mp$ 0.013	$\pm$ 0.002	$\mp$ 0.014	$\mp$ 0.037
$\rm B_s$ fraction	$\pm$ 0.058	$\pm$ 0.048	$\pm$ 0.047	$\pm$ 0.062
Barions fraction	$\mp$ 0.013	$\mp$ 0.026	$\pm$ 0.043	$\pm$ 0.057
Mixing in b $\rightarrow$ X$\ell\nu$	$\pm$ 0.037	-	$\mp$ 0.058	-
Mixing in b $\rightarrow$ c $\rightarrow$ X$\ell\nu$	$\mp$ 0.054	-	$\pm$ 0.084	-
c charge tag rate	$\pm$ 0.043	-	$\mp$ 0.067	-
charge correlation	$\pm$ 0.079	-	$\mp$ 0.123	-
bkg charge correlation	$\pm$ 0.027	-	$\mp$ 0.042	-
$\epsilon_{\rm c}$ sample $\mathcal{B}$	$\pm$ 0.014	$\pm$ 0.026	$\pm$ 0.010	$\mp$ 0.009
$\epsilon_{\rm x}$ sample $\mathcal{B}$	$\pm$ 0.015	$\pm$ 0.015	$\pm$ 0.011	$\pm$ 0.012
$\epsilon_{\rm c}$ sample $\mathcal{J}$	$\mp$ 0.018	-	$\pm$ 0.028	-
$\epsilon_{\rm x}$ sample $\mathcal{J}$	negl	-	negl	-
$\epsilon_{\rm c}$ sample $\mathcal{P}$	$\mp$ 0.012	-	$\pm$ 0.018	-
$\epsilon_{\rm x}$ sample $\mathcal{P}$	negl	-	negl	-
Total	$\pm$ 0.298	$\pm$ 0.159	$\pm$ 0.239	$\pm$ 0.423

Table 2: Estimated contributions to the systematic uncertainty on BR(b $\rightarrow$ X$\ell\nu$) and BR(b $\rightarrow$ c $\rightarrow$ X$\ell\nu$). Results for both transverse momentum and charge correlation analysis are given. Uncertainties from modelling are shown separately in the next table. All the results are given in percent units.

	Δ[BR(b $\to$ X$\ell\nu$)]		Δ[BR(b $\to$ c $\to$ X$\ell\nu$)]	
Modelling	Charge	$p_\perp$	Charge	$p_\perp$
b $\to$ X$\ell\nu$	$\pm$ 0.133	$\pm$ 0.371	$\pm$ 0.022	$\pm$ 0.383
c $\to$ ℓ	$^{-0.037}_{+0.021}$	$^{-0.086}_{+0.071}$	$^{-0.114}_{+0.061}$	$^{-0.037}_{+0.020}$
b $\to$ D	$^{-0.002}_{+0.001}$	$^{-0.071}_{+0.060}$	$^{-0.057}_{+0.049}$	$^{+0.055}_{-0.049}$
Total	$^{+0.134}_{-0.138}$	$^{+0.383}_{-0.388}$	$^{+0.081}_{-0.129}$	$^{+0.387}_{-0.388}$

Table 3: Estimated systematic uncertainties due to modelling

[5] B. Mours *et al.*, Nucl. Instr. Meth. A **379** (1996) 101.

[6] ALEPH Coll., R. Barate *et al.*, “Measurement of the effective b quark fragmentation function at the Z peak”, ALEPH/2000-068, CONF/2000-046, Contribution to ICHEP 2000, abstract 173, paper 134.

[7] ALEPH Coll., D. Buskulic *et al.*, Z. Phys. C **60** (1993) 71.

[8] ALEPH Coll., R. Barate *et al.*, Phys. Lett. B **401** (1997) 150-162.

[9] ALEPH Coll. R. Barate *et al.*, Nucl. Instr. Meth. A **346** (1994) 461.

[10] LEP/SLD Heavy Flavour Working Group, Input Parameters for the LEP Electroweak Heavy Flavour Results for Summer 1998 Conferences, LEPHF/98-01.

[11] ALEPH, DELPHI, L3, OPAL and SLD Collabs., “Combined results on b-hadron production rates, lifetimes, oscillations and semileptonic decays”, SLAC–PUB/8492, CERN–EP/2000–096

[12] LEP/SLD Electroweak Working Group, A Combination of Preliminary Electroweak Measurements and Constraints on the Standard Model, prepared from contributions of the LEP and SLD experiments to the 1999 Summer conferences, CERN-EP preprint in preparation.

[13] C. Peterson, D. Schlatter, I. Schmitt and P.M. Zerwas, Phys. Rev. D **27** (1983) 105.

[14] The LEP Collabs., ALEPH, DELPHI, L3 and OPAL, Nucl., Instr. Meth. A **378** (1996) 101.

[15] DELCO Coll.,W. Bacino *et al.*, Phys. Rev. Lett. **43** (1979) 1073

[16] MARK III Coll., R. M. Baltrusaitis *et al.*, Phys. Rev. Lett. **54** (1985) 1976

[17] CLEO Coll., S. Henderson *et al.*, Phys. Rev. Lett. D **45** (1992) 2212